

# Kinetic freeze out conditions in nuclear collisions with 2 – 158A GeV beam energy within a non boost-invariant blast wave model

Sudhir Pandurang Rode,<sup>1</sup> Partha Pratim Bhaduri,<sup>2</sup> Amaresh Jaiswal,<sup>3</sup> and Ankhi Roy<sup>1</sup>

<sup>1</sup>*Discipline of Physics, School of Basic Sciences,  
Indian Institute of Technology Indore, Indore 453552 India*

<sup>2</sup>*Variable Energy Cyclotron Centre, HBNI, 1/AF Bidhan Nagar, Kolkata 700 064, India*

<sup>3</sup>*School of Physical Sciences, National Institute of Science Education and Research, HBNI, Jatni-752050, Odisha, India*  
(Dated: March 22, 2019)

We study the kinetic freeze out conditions of bulk hadrons in nuclear collisions. The transverse and longitudinal momentum spectra of the identified hadrons produced in central Au+Au and Pb+Pb collisions, in the beam energy range of  $E_b = 2 - 158$  A GeV are analysed for this purpose, within a generalised non boost-invariant blast wave model. The kinetic freeze out temperature is found to vary in the range of 55 - 90 MeV, whereas the average transverse velocity of collective expansion is found to be around  $0.5c$  to  $0.6c$ . The mean longitudinal velocity of the fireball is seen to increase monotonically with increasing longitudinal boost. The results would be useful to understand the gross collision dynamics for the upcoming experiments at the FAIR and NICA accelerator facilities.

## I. INTRODUCTION

One of the major objectives of the relativistic heavy ion collision research program is to explore the phase structure of the strongly interacting matter [1–3]. Regions of temperature and baryon density that can be accessed in a particular experiment, depend on the collision energy. Thus systems with very small net baryon densities but rather high temperature are formed at top Relativistic Heavy Ion Collider (RHIC) and Large Hadron Collider (LHC) energies. Data collected by the experiments at these two collider facilities [4–8] have provided conclusive evidence for the formation of strongly coupled Quark Gluon Plasma (QGP) [9]. Compared to this nuclear phase diagram is much less explored in the region of high net baryon densities. Relativistic nuclear collisions at moderate energies such as those operating at RHIC Beam Energy Scan (BES) program or those becoming available at upcoming FAIR accelerator facility at GSI, Germany [10] or NICA facility at JINR, Dubna [11], are expected to create hot and dense nuclear matter in the regime of moderate temperature and large net baryon density.

For optimum utilisation of these facilities, to explore the phase structure, it is imperative to analyse the existing data sets in the similar energy range, collected by the fixed target experiments at AGS and SPS accelerator facilities. In particular, it is important to know what thermodynamic environments are being generated in the bulk of the collision systems at various bombarding energies. Due to technological limitations related to beam intensities, the experiments are mostly limited to the measurement of soft probes that constitute bulk of the excited matter produced in the collisions. Soft hadronic observables measure directly the final “freeze-out” stage of the collision, when hadrons decouple from the bulk and free-stream to the detectors. They exhibit a strong collective behaviour that can be analysed within the ambit of rel-

ativistic hydrodynamics [12, 13].

Apart from hydrodynamics, the observables pertaining to collective behaviour of the nuclear fireball can also be studied using the hydrodynamics inspired so-called blast wave model [14]. Blast wave models are in vogue for a long time to analyse momentum distribution of the produced hadrons and provide information about the properties of the matter at kinetic freeze-out. The main underlying assumption is that the particles in the system produced in the collisions are locally thermalised (till they are emitted from the medium) and the system expands collectively with a common radial velocity field undergoing an instantaneous common freeze-out. Such phenomenological models are particularly useful in the nuclear collisions, where a fireball is created with finite net baryon density, as the hydrodynamic calculations in the corresponding regime, suffer from the unavailability of realistic equation of states from lattice QCD.

The first version of blast wave model was formulated about four decades ago [15], to describe the hadron production in Ne+NaF reactions at a beam energy of 800 A MeV. The model assumes the spherically symmetric expansion of shells of matter with constant radial velocity. Collective isentropic expansion of the nuclear fireball with a scaling form for the radial velocity profile was also used to analyse the then available data on transverse momentum ( $p_T$ ) spectra of hadrons from 14.5 A GeV Si+Au collisions at BNL AGS and 200 A GeV O+Au collisions at CERN SPS [16, 17].

While the spherically expanding source may be expected to mimic the fireball created at low energies, at higher energies stronger longitudinal flow might lead to cylindrical geometry. For the latter case an appropriate formalism was first developed in Ref. [18]. Using a simple functional form for the phase space density at kinetic freeze out, the authors approximated the hydrodynamical results with boost-invariant longitudinal flow. The model was successfully used to fit the  $p_T$  spectra with

only two parameters namely a kinetic freeze-out temperature  $T_{kin}$  and a radial flow strength  $\beta_T$ . Though initially developed for central collisions, the model was later extended to non-central collisions with introduction of additional parameters to account for anisotropies in the transverse flow profile [19] and in the shape of the source in the co-ordinate space [20]. The model has also been applied to search for collectivity in small systems [21]. Attempts have also been made to incorporate the viscous effects in the blast wave model [22, 23]. One common assumption for all these variants of the blast wave model is the underlying boost-invariant longitudinal dynamics. Though a reasonable assumption at RHIC and LHC energies, longitudinal boost-invariance does not hold well at AGS and SPS energies. Thus to describe particle production in these energy domain requires models where assumption of boost-invariance is relaxed.

In Ref. [24], the authors proposed a non boost-invariant extension of the blast wave model of [18], in the minimal way by modifying the system boundaries, suitable for low energy collisions. For a realistic parametrisation of the freeze out surface of the expanding fireball, the model has been found to provide a very good fit to the  $p_T$  and rapidity spectra for a variety of hadrons produced in 11.6 A GeV Au+Au collisions measured by E802, E877 and E891 Collaborations at AGS. The results indicated a relatively low kinetic freeze-out temperature of about 90 MeV with an average transverse expansion velocity at mid-rapidity of about  $0.5c$ . In the present article, we follow the same recipe to analyse the transverse and longitudinal spectra of the bulk hadrons from Au+Au and Pb+Pb collisions in the energy range  $E_b = 2 - 158$  A GeV, as measured by different experimental Collaborations at AGS and SPS and RHIC facilities. The results of our investigations help to improve the understanding of the gross features of the collision dynamics in this energy domain which is certainly useful for the second generation experiments at FAIR and NICA accelerator facilities.

## II. A BRIEF DESCRIPTION OF THE MODEL

Details of the non boost-invariant blast wave model that we have employed in our calculations can be found in [24]. Here we briefly outline the main features for completeness. In blast wave models, the single particle momentum spectrum of the hadrons emitted from the fireball at freeze out are usually described by Cooper Frye [25] prescription of particle production. Within this formalism, the single particle spectrum is defined as the integral of the phase space distribution function  $f(x, p)$  over the freeze-out hyper-surface  $\Sigma_\mu^f(x)$ . The triple differential invariant spectra can be written as:

$$E \frac{d^3 N}{d^3 p} = \frac{g}{2\pi^3} \int d^3 \Sigma_\mu^f(x) p^\mu f(x, p) \quad (1)$$

where  $g$  denotes the degeneracy factor. In thermal models,  $f(x, p)$  is considered to be the equilibrium distribu-

tion function. In the temperature range of the heavy-ion collisions, the quantum statistics can be ignored and one usually works with Boltzmann approximation. The freeze-out hyper surface  $\Sigma_\mu^f(x)$  is determined from freeze out criterium for thermal decoupling.

For an expanding fireball under local thermal equilibrium, the boosted thermal distribution is given by:

$$f(x, p) = \exp \left( -\frac{p \cdot u(x) - \mu(x)}{T(x)} \right) \quad (2)$$

where  $T(x)$  and  $\mu(x)$  are space time dependent local temperature and chemical potentials at kinetic freeze out and  $u^\mu(x) = \gamma(1, \beta_T(x)e_r, \beta_L(x))$  is the local fluid velocity. Focusing on central collisions, with a realistic parametrisation of the freeze-out hyper-surface and local fluid velocity, the thermal single particle spectrum in terms of transverse mass  $m_T (= \sqrt{p_T^2 + m^2})$  and rapidity  $y$  read as:

$$\begin{aligned} \frac{dN}{m_T dm_T dy} &= \frac{g}{2\pi} m_T \tau_F \int_{-\eta_{max}}^{+\eta_{max}} d\eta \cosh(y - \eta) \\ &\times \int_0^{R(\eta)} r_\perp dr_\perp I_0 \left( \frac{p_T \sinh \rho(r_\perp)}{T(x)} \right) \\ &\times \exp \left( \frac{\mu(x) - m_T \cosh(y - \eta) \cosh \rho(r_\perp)}{T(x)} \right). \end{aligned} \quad (3)$$

where the system is assumed to undergo an instantaneous common freeze-out at a proper time  $\tau = \sqrt{t^2 - z^2} = \tau_F$ . In the above equation,  $\eta = \tanh^{-1}(z/t)$  denotes the space-time rapidity and is related to the longitudinal fluid velocity via  $\beta_L = \tanh(\eta)$ . In the transverse plane the flow rapidity (or transverse rapidity)  $\rho$  is related to the collective transverse fluid velocity,  $\beta_T$ , via the relation  $\beta_T = \tanh(\rho)$ .

Considering a Hubble like expansion of the fireball in the transverse plane, a radial dependence of the transverse fluid velocity has been assumed of the form

$$\beta_T(r) = \beta_T^0 \left( \frac{r_\perp}{R} \right)^n. \quad (4)$$

where  $\beta_T^0$  is the transverse fluid velocity at the surface of the fireball. The average transverse flow velocity, for such a scaling form is given by,  $\langle \beta_T \rangle = \frac{2}{2+n} \beta_T^0$ . The transverse flow vanishes at the centre and assumes maximum value at the edges, with the flow profile decided by value of  $n$ . Most hydrodynamic calculations suggest  $n = 1$  leading to a transverse rapidity flow field linear in the radial coordinate [26]. Such linear parametrization essentially leads to an exponential expansion of the fireball in the transverse direction, hence the name blast wave.

To account for the limited available beam energy, the longitudinal boost-invariant scenario is modified by restricting the boost angle  $\eta$  to the interval  $\eta_{min} \leq \eta \leq \eta_{max}$ . Reflection symmetry about centre of mass ensures  $\eta_{min} = -\eta_{max}$  and thus constrains the freeze out volume up to a maximum space time rapidity  $\eta_{max}$ . In the transverse plane the boundary of the fireball is given by

TABLE I: Details of the data sets from different experiments at different accelerator facilities along with energy ( $E_{lab}$ ), beam rapidity ( $y_b$ ), System, Centrality, Phase space and hadron species, used for blast wave analysis.

Facility	Experiment	$E_{lab}$ (A GeV)	$y_b$	System	Centrality	Phase space	Hadron Species
AGS	E895	2 [29] [30]	1.39	Au+Au	0 – 5%	$-0.05 < y_{c.m.} < 0.05$	$\pi^+, \pi^-, p$
AGS	E895	4	2.13	Au+Au	0 – 5%	$-0.05 < y_{c.m.} < 0.05$	$\pi^+, \pi^-, p$
AGS	E895	6	2.54	Au+Au	0 – 5%	$-0.05 < y_{c.m.} < 0.05$	$\pi^+, \pi^-, p$
AGS	E895	8	2.83	Au+Au	0 – 5%	$-0.05 < y_{c.m.} < 0.05$	$\pi^+, \pi^-, p$
SPS	NA49	20 [32]	3.75	Pb+Pb	0 – 7%	$0.0 < y_{c.m.} < 0.2 (\pi^-)$ $-0.1 < y_{c.m.} < 0.1 (k^\pm)$ $-0.38 < y_{c.m.} < 0.32 (p)$	$\pi^-, k^\pm, p$
RHIC BES	STAR	30.67 [31]	4.18	Au+Au	0 – 5%	$-0.1 < y_{c.m.} < 0.1$	$\pi^\pm, k^\pm, p, \bar{p}$
SPS	NA49	30	4.16	Pb+Pb	0 – 7%	$0.0 < y_{c.m.} < 0.2 (\pi^-)$ $-0.1 < y_{c.m.} < 0.1 (k^\pm)$ $-0.48 < y_{c.m.} < 0.22 (p)$	$\pi^-, k^\pm, p$
SPS	NA49	40 [33]	4.45	Pb+Pb	0 – 7%	$0.0 < y_{c.m.} < 0.2 (\pi^-)$ $-0.1 < y_{c.m.} < 0.1 (k^\pm)$ $-0.32 < y_{c.m.} < 0.08 (p)$	$\pi^-, k^\pm, p$
RHIC BES	STAR	69.56	5.00	Au+Au	0 – 5%	$-0.1 < y_{c.m.} < 0.1$	$\pi^\pm, k^\pm, p, \bar{p}$
SPS	NA49	80	5.12	Pb+Pb	0 – 7%	$0.0 < y_{c.m.} < 0.2 (\pi^-)$ $-0.1 < y_{c.m.} < 0.1 (k^\pm)$ $-0.36 < y_{c.m.} < 0.04 (p)$	$\pi^-, k^\pm, p$
SPS	NA49 [34]	160	5.82	Pb+Pb	0 – 7%	$0.0 < y_{c.m.} < 0.2 (\pi^-)$ $-0.1 < y_{c.m.} < 0.1 (k^\pm)$ $-0.51 < y_{c.m.} < -0.11 (p)$	$\pi^-, k^\pm, p$

$R(\eta)$ . Two different choices of  $R(\eta)$  are prescribed in [24], corresponding to different shapes of the fireball:

$$R(\eta) = R_0 \cdot \Theta(\eta_{\max}^2 - \eta^2), \quad (5)$$

$$R(\eta) = R_0 \cdot \sqrt{1 - \frac{\eta^2}{\eta_{\max}^2}}. \quad (6)$$

The first choice, Eq. (5) describes a cylindrical fireball in the  $\eta - r_\perp$ -space and corresponds to the usual formalism [18], which was found to work well at top SPS energies and above. However at lower AGS beam energy, the cylindrical symmetry is not fully realised and the fireball is expected to have an elliptic shape [27], as given by Eq. (6). Dependence of transverse size on the longitudinal coordinate explicitly breaks the assumption of boost-invariance.

While analysing the AGS data, the authors of Ref. [24] had investigated a wide range of possibilities for the different freeze-out parameters. Comparison between fit

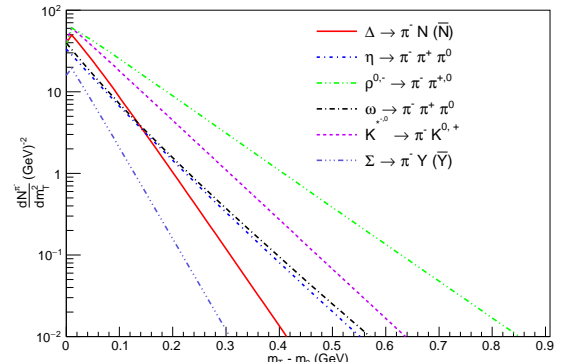


FIG. 1: An illustration of the resonance decay contributions to the transverse mass spectra of pions. Both two and three body decays are incorporated in the calculation. Higher mass resonances beyond  $\Delta(1232)$  are neglected.

TABLE II: Summary of the fit results at different energies from AGS, SPS and RHIC beam energy scan (BES). For uniformity, at RHIC the relevant centre of mass (CMS) energies are converted to the corresponding beam energies in the laboratory frame.

$E_b$ (A GeV)	$\eta_{max}$	$\langle\beta_T\rangle$	$T_{kin}$ (MeV)	$\chi^2/\text{NDF}$
2	$0.995 \pm 0.001$	$0.4838 \pm 0.0034$	$61.72 \pm 1.36$	7.2
4	$1.285 \pm 0.002$	$0.5400 \pm 0.0025$	$55.86 \pm 1.38$	7.8
6	$1.573 \pm 0.002$	$0.5584 \pm 0.0062$	$58.14 \pm 3.17$	9.4
8	$1.645 \pm 0.003$	$0.5655 \pm 0.0031$	$60.63 \pm 1.75$	8.7
20	$1.882 \pm 0.005$	$0.5177 \pm 0.0011$	$79.77 \pm 0.05$	6.5
30.67	$2.078 \pm 0.004$	$0.5448 \pm 0.0002$	$71.25 \pm 0.02$	8.5
30	$2.084 \pm 0.004$	$0.5368 \pm 0.0011$	$80.28 \pm 0.05$	6.7
40	$2.094 \pm 0.004$	$0.5356 \pm 0.0009$	$81.92 \pm 0.04$	5.5
69.56	$2.306 \pm 0.005$	$0.5330 \pm 0.0001$	$78.97 \pm 0.01$	6.7
80	$2.391 \pm 0.005$	$0.5347 \pm 0.0012$	$82.68 \pm 0.05$	3.8
158	$2.621 \pm 0.006$	$0.538 \pm 0.0013$	$84.11 \pm 0.06$	4.4

quality and the number of model parameters (and the related expense in computing time) showed an optimum description of the both longitudinal and transverse spectra can be obtained by reducing the transverse size of the fireball in backward and forward rapidity regions, following Eq. (6), along with a temperature and transverse flow gradient constant over the freeze out surface. In our present analysis, we would thus opt for the same parametrisation for describing the longitudinal and transverse spectra.

For comparison to experimental data, one needs to account for hadronic resonance decays. In our calculations, we do so following [28] using thermal distributions Eq. (3) for the resonances. Both two and three body decay of the sources are numerically simulated. The procedure implies the assumption of full chemical equilibrium which is sufficient for estimating the resonance feed down contributions. The resonance decay contributions to the pion spectra are illustrated in Fig. 1. We only include hadrons with masses up to  $\Delta(1232)$  resonance. As our analysis is restricted up to SPS energies, exclusion of higher resonances would have a negligible effect.

### III. RESULTS AND DISCUSSIONS

In this section we present the results of our analysis. For this purpose we consider the measured spectra of the identified hadrons in central Au+Au collisions from E895 Collaboration [29, 30] at AGS in the beam energy range  $E_b = 2 - 8$  A GeV and from STAR Collaboration at RHIC BES program [31] for two centre of mass energies  $\sqrt{s_{NN}} = 7.7$  and 11.5 GeV ( $E_b = 30.67$  and 69.56 A GeV). In addition data for central Pb+Pb collisions from

NA49 Collaboration [32–34] at SPS, in the beam energy range  $E_b = 20 - 158$  A GeV are analysed. We do not go beyond top SPS energy. Note that at AGS the distribution of secondary hadrons were measured by a series of experiments at varying energies and for various collision systems. For the present analysis, we only opt for the latest available data corpus for central Au+Au collisions, from E895 Collaboration. The data were published as acceptance corrected, invariant yield per event as a function of  $m_T - m_0$  ( $m_0$  being the particle mass), in small bins of rapidity ( $\Delta y = 0.1$ ). For uniformity, in our analysis we consider only the mid rapidity bin, where the yield is maximum. For most forward/backward rapidity bins data points are mostly not available at higher  $p_T$ . The details of the data sets under investigation, including their beam energy, beam rapidity, collision centrality, phase space coverage and analysed hadronic species are summarised in Table I. As we are interested in the global properties of the fireball, we consider only bulk hadronic species namely pions ( $\pi^-, \pi^+$ ) and protons ( $p$ ) at AGS energies, ( $\pi^\pm, K^\pm$  and  $p, \bar{p}$ ) at RHIC beam energy scan (BES) program energies and pions ( $\pi^-$ ), kaons ( $K^+, K^-$ ) and protons ( $p$ ) at SPS energies. Due to a lower  $p_T$  cut off ( $p_T^{min} \simeq 0.2$  GeV), the resonance decay contribution is excluded while fitting the spectra from RHIC BES program.

We start by fitting the  $p_T$  distribution of identified hadrons using Eq. (3) at different energies. To keep the number of fitting parameters minimal, we couple the freeze out time  $\tau_F$ , degeneracy factor  $g$  and the fugacity (chemical potential) together into a single normalisation constant  $Z = \frac{g}{2\pi} \tau_F \exp(\mu/T)$ , which is adjusted separately for different particle species. Note that the value of chemical potential is fixed at chemical freeze-out and

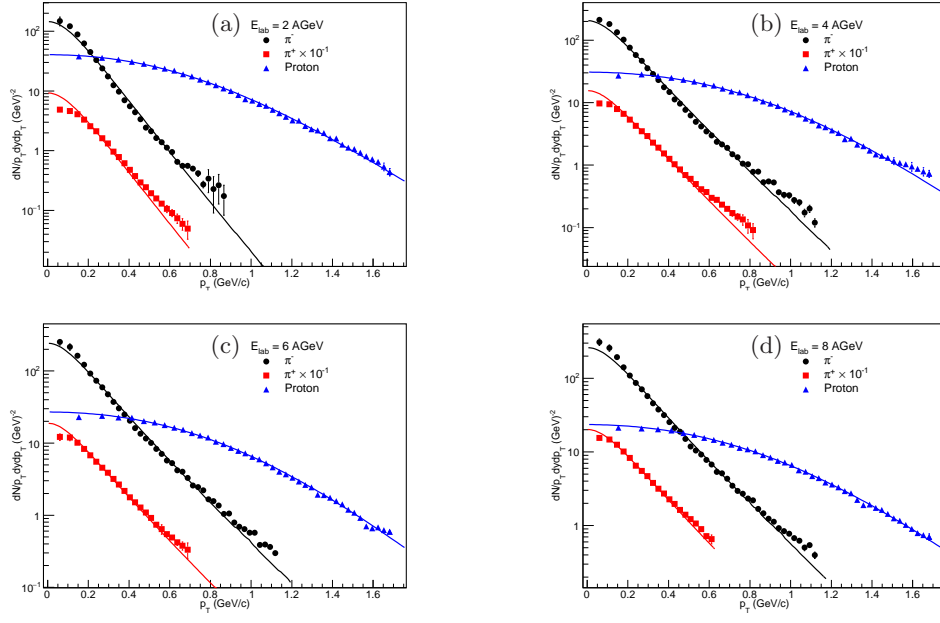


FIG. 2: Fitted  $p_T$  spectra for Pions ( $\pi^\pm$ ) ( $-0.05 < y_{cm} < 0.05$ ), and Proton ( $-0.05 < y_{cm} < 0.05$ ) at (a) 2 AGeV, (b) 4 AGeV, (c) 6 AGeV and (d) 8 AGeV beam energies.

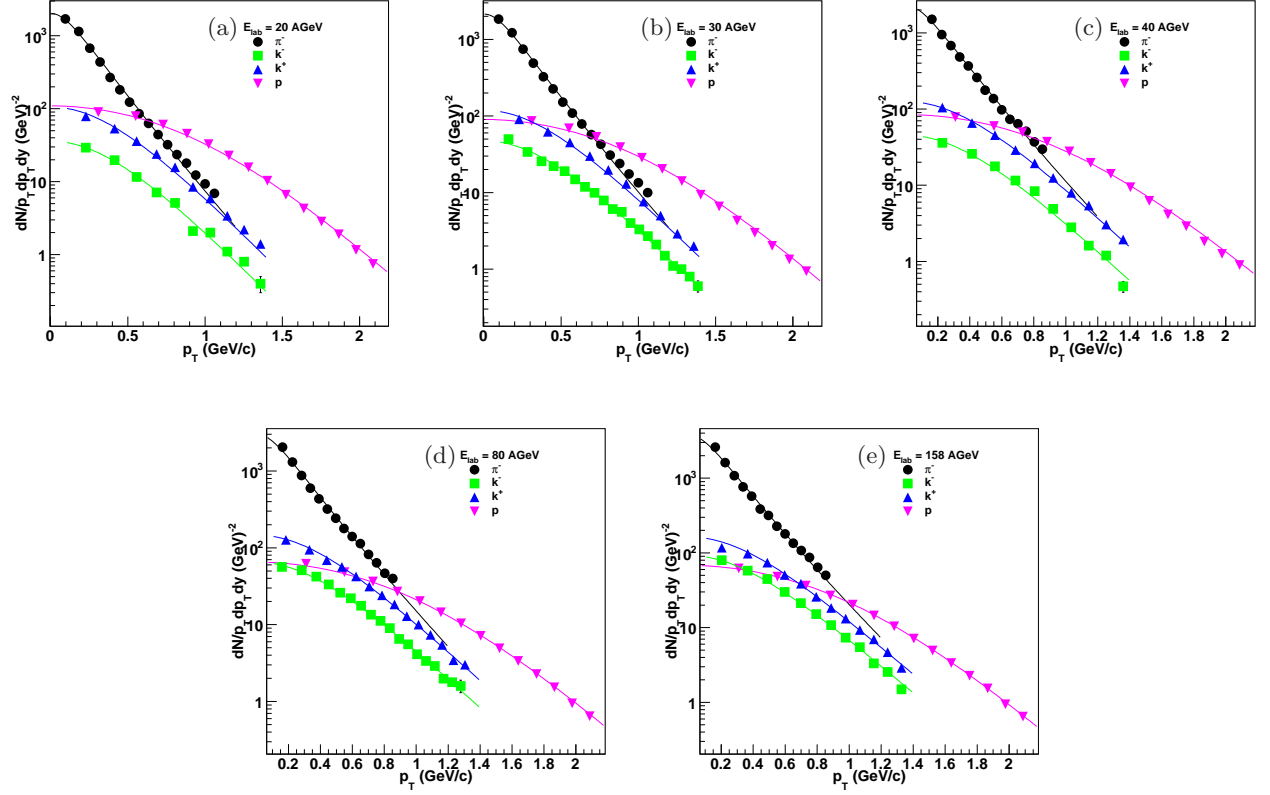


FIG. 3: Fitted  $p_T$  spectra for proton ( $-0.38 < y_{cm} < 0.32$  for 20 AGeV,  $-0.48 < y_{cm} < 0.32$  for 30 AGeV,  $-0.32 < y_{cm} < 0.08$  for 40 AGeV,  $-0.36 < y_{cm} < 0.04$  for 80 AGeV and  $-0.51 < y_{cm} < -0.11$  for 158 AGeV),  $\pi^\pm$  ( $0.0 < y_{cm} < 0.2$ ) and  $K^\pm$  ( $-0.1 < y_{cm} < 0.1$ ) at (a) 20 AGeV, (b) 30 AGeV, (c) 40 AGeV, (d) 80 AGeV and (e) 158 AGeV beam energies.

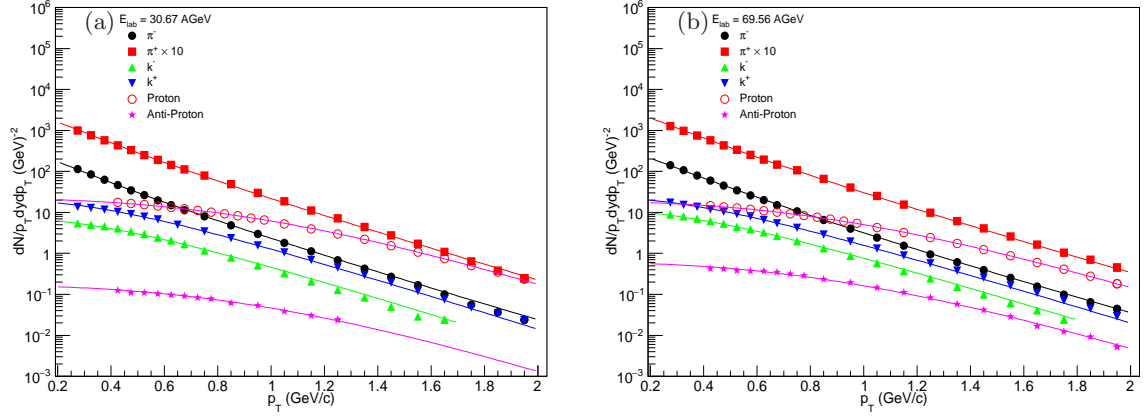


FIG. 4: Fitted  $p_T$  spectra for proton ( $-0.1 < y_{cm} < 0.1$ ), antiproton ( $-0.1 < y_{cm} < 0.1$ ),  $\pi^\pm$  ( $0.1 < y_{cm} < 0.1$ ),  $K^\pm$  ( $-0.1 < y_{cm} < 0.1$ ) and  $K^\pm$  ( $-0.1 < y_{cm} < 0.1$ ) from RHIC beam energy scan (BES) program, at (a) 30.67 AGeV and (b) 69.56 AGeV beam energies. Since the data have a lower  $p_T$  cut off around 200 MeV, the resonance decay contribution is not included in the calculations.

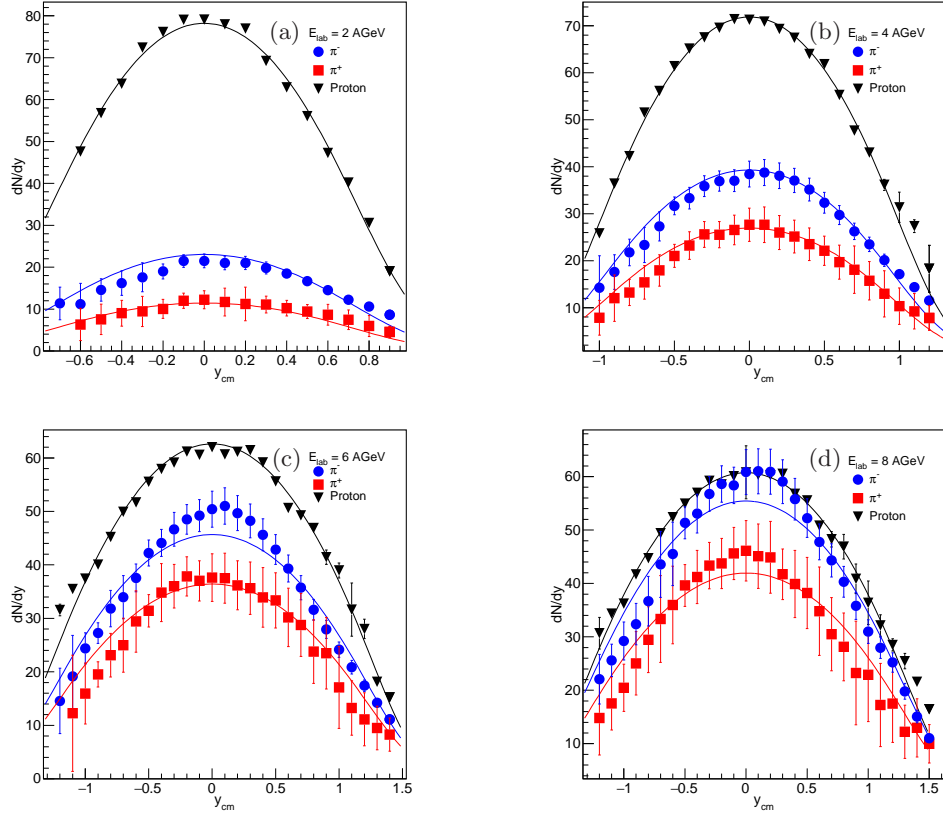


FIG. 5: Fitted rapidity distribution of  $\pi^\pm$  and Proton in central Au+Au collisions from AGS, at (a) 2 AGeV, (b) 4 AGeV, (c) 6 AGeV and (d) 8 AGeV beam energies. For each particle species the normalisation has been adjusted separately for best fit results.



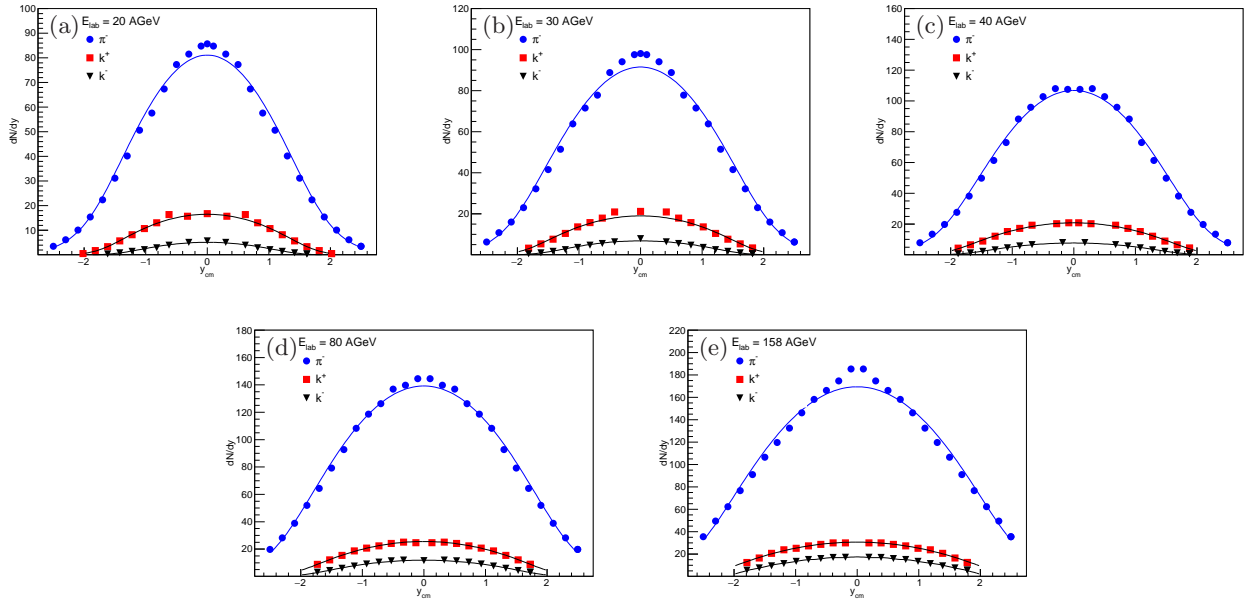


FIG. 6: Fitted rapidity distribution of  $\pi^-$ ,  $K^+$  and  $K^-$  in central Pb+Pb collisions from SPS, at (a) 20 AGeV, (b) 30 AGeV, (c) 40 AGeV, (d) 80 AGeV and (e) 158 AGeV beam energies.

hence its absorption inside the normalisation would not affect the thermodynamic conditions at kinetic freeze-out. For a given transverse flow profile ( $n = 1$ ), we are thus essentially left with three parameters namely  $T$ ,  $\eta_{max}$  and  $\beta_T^0$  which are common for all hadrons at a given energy and extracted from the simultaneous fitting of the  $p_T$  spectra of selected hadronic species. The extracted parameters are then used to describe the rapidity spectra of those particles. The resulting  $p_T$  spectra at AGS, SPS and RHIC BES are shown in Fig. 2, 3 and 4 respectively. The corresponding best fitted values of the parameters  $\eta_{max}$ ,  $\langle\beta_T\rangle$  and  $T_{kin}$  at different beam energies, obtained via minimization of reduced  $\chi^2$  (defined as  $\chi^2$  per degree of freedom) are given in the Table II.

As evident the model gives a reasonable description of the  $p_T$  spectra of the bulk hadrons at all investigated energies. The freeze out temperature is found to be relatively low which gradually increases with beam energy. Rather a strong transverse collective motion is observed even at lowest AGS energy. Hadronic  $p_T$  spectra, in this investigated energy domain has also been analysed within the boost-invariant blast wave model. Relatively higher freeze out temperatures ( $T_{kin} > 100$  MeV) has been observed even at AGS energies with a slightly weaker transverse flow [35]. However one should take note of the fact, that in the corresponding analysis particles are chosen above a non zero  $p_T$  value (eg: 0.5 GeV/c for pions) to exclude the effect of resonance decay. Also the transverse flow parameter  $n$  is kept free (which is about 0.5) and fixed from the data whereas we set it to  $n = 1$ .

In this context we would also like to mention that at AGS previous attempts had been also made to fit the transverse distribution of the hadrons with a static rapidity dependent two slope empirical model in absence

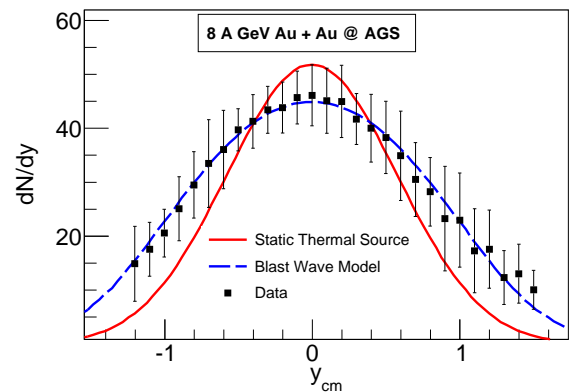


FIG. 7: Rapidity density distributions of pions in 8 A GeV central Au+Au collisions at AGS. Data are compared with predictions from a static thermal model and non boost-invariant blast wave model.

of any collective flow [29]. The two inverse slope parameters  $T_1$  and  $T_2$  respectively dominate the low and high end of the  $m_T - m_0$  spectra. Both  $T_1$  and  $T_2$  assume maximum values at mid rapidity, with  $T_1$  around 50 MeV and  $T_2$  around 130 MeV.

After successful description of the  $p_T$  spectra, we now move on to the description of the rapidity distribution of the produced hadrons. Longitudinal spectra are useful to explore the collective effects in the longitudinal direction. Integrating Eq. (3) over the transverse components we obtain the rapidity distribution which is contrasted with the available data from AGS and SPS. No data on rapidity distribution of the bulk hadrons, is available from RHIC BES program. The same  $\eta_{max}$  values as listed in

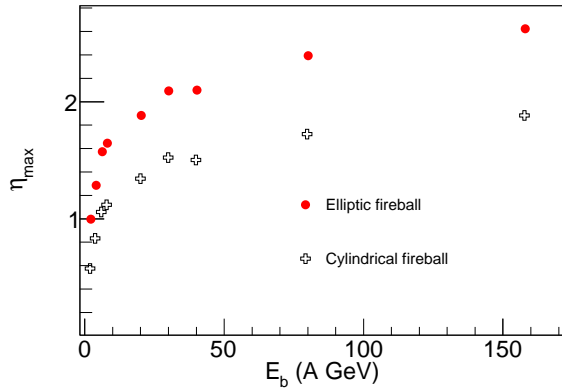


FIG. 8: Comparison of the  $\eta_{max}$  values for different beam energies at AGS and SPS for an elliptic fireball and a cylindrical fireball. The value  $\eta_{max}$  is consistently larger for former case compared to the latter one.

Table II are now used to describe the rapidity density distributions. However the freeze out temperatures  $T_{kin}$  are not chosen from the fit to the  $p_T$  spectra. The  $p_T$  spectra are fitted only in the mid-rapidity region. In a non boost invariant model, the physical quantities, including the temperature would depend on the rapidity of the measured hadrons. One might also recall that rapidity spectra are rather insensitive to the underlying temperature [18]. Change of temperature has a minimal effect on the corresponding value of  $\eta_{max}$ . Temperature values as high as 120 – 150 MeV can also describe the observed rapidity distributions of the produced particles. In our calculations, we fix  $T_{kin}$  to 120 MeV which gives a reasonable fit to the rapidity spectra. However such high values of temperature can not provide a reasonable fit to the  $p_T$  spectra. The results are depicted in Fig. 5 and 6.

The rapidity distribution of a particle of mass  $m$ , emitted from a static thermal source at temperature  $T$  has the form

$$\frac{dn_{th}}{dy} = \frac{V}{(2\pi)^2} T^3 \left( \frac{m^2}{T^2} + \frac{m}{T} \frac{2}{\cosh y} + \frac{2}{\cosh^2 y} \right) \times \exp \left( -\frac{m}{T} \cosh y \right) \quad (7)$$

where  $V$  denotes the source volume. It is well known that static isotropic thermal emission models applied to observed particle rapidity distributions from experiments at all beam energies consistently fail to describe the observed shape; such model predictions being too narrow. Thermal models which include collective longitudinal expansion have been much more successful at reproducing the observed rapidity distributions. An illustrative comparison is presented in Fig. 7, where rapidity distribution of the pions in 8 A GeV central Au+Au collisions is contrasted with that from a static thermal model as well as from the present blast wave model calculations. As evident rapidity distribution from a static isotropic thermal source falls much faster than the data. Similar feature is

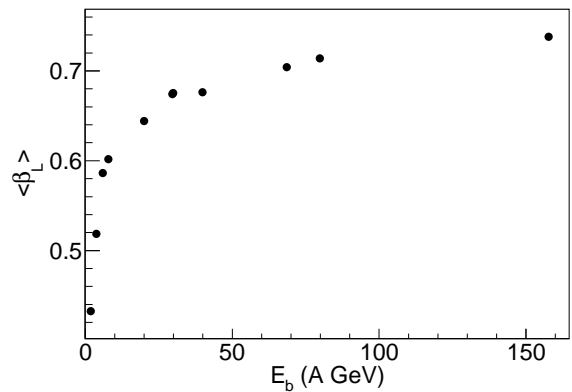


FIG. 9: Variation of the average longitudinal velocity of the fireball with beam energy.

observed for all other particles and at all the investigated energies. The additional collective motion is attributed to intense pressure gradients which develop in the very hot, compressed nuclear matter fireballs created in heavy ion collisions. Note that the longitudinal flow is generally incorporated with a longitudinally boost-invariant superposition of multiple boosted individual isotropic, locally thermalised sources in a given rapidity interval [36]. Each locally thermalised source is modeled by the  $m_T$  - integrated Maxwell-Boltzmann distribution, with the rapidity dependence of the energy,  $E = m_T \cosh y$  explicitly included. Thus within a boost-invariant scenario, the rapidity distribution from a boosted thermal source can be written as

$$\frac{dn}{dy}(y) = \int_{\eta_{min}}^{\eta_{max}} d\eta \frac{dn_{th}}{dy}(y - \eta) \quad (8)$$

Note that Eq. (8) is equivalent to what we obtain by integrating Eq. (3) over  $p_T$ , for a cylindrical fireball as given by Eq. (5). For comparison, we independently fit the rapidity distribution of pions for both  $\eta$  dependent and  $\eta$  independent transverse radius of the fireball. A comparison of the extracted values of  $\eta_{max}$  at different energies, for elliptic fireball and cylindrical fireball, is displayed in Fig. 8. For the non boost-invariant model  $\eta_{max}$  (and hence the maximum longitudinal fluid velocity) is consistently higher than a boost-invariant case.

In closing it might also be interesting to investigate the effect of longitudinal flow within the present model. For a cylindrical fireball, in the flat portion of the rapidity distribution, one can define an average longitudinal velocity as  $\langle \beta_L \rangle = \tanh(\eta_{max}/2)$  [36]. Note that the longitudinal velocity  $\beta_L$  is not a linear function of  $\eta$  and therefore the above expression for  $\langle \beta_L \rangle$  may not hold for non boost-invariant models. For non boost-invariant models, the longitudinal and transverse motion of the thermal source can no longer be decoupled. The rapidity distribution is no longer flat in  $\eta$  within the region  $\eta_{min} < \eta < \eta_{max}$ . One can still define an average of the magnitude of lon-



gitudinal velocity of the medium as

$$\langle\beta_L\rangle = \frac{\int_0^{\eta_{\max}} d\eta \tanh(\eta)}{\int_0^{\eta_{\max}} d\eta} = \frac{\ln(\cosh \eta_{\max})}{\eta_{\max}}.$$

From the above expression, we see that  $\langle\beta_L\rangle \rightarrow 1$  as  $\eta_{\max} \rightarrow \infty$ . Note that, as  $\eta_{\max} \rightarrow \infty$ , longitudinal boost-invariance symmetry is restored. The dependence of  $\langle\beta_L\rangle$  with  $E_b$  is shown in Fig. 9. We observe that  $\langle\beta_L\rangle$  initially increases and gradually shows a saturative trend with increasing beam energy. This is a consequence of the result shown in Fig. 8 where we find that the fitted value of  $\eta_{\max}$  increases as the beam energy is increased. Therefore, from our analyses of beam energy dependence of  $\eta_{\max}$  and  $\langle\beta_L\rangle$ , we conclude that longitudinal boost-invariance is expected to be recovered at high collision energies.

One may also note that since the protons are present before the collision, they are subject to nuclear transparency effect, which is not incorporated in our calculations. At higher beam energies the effect might be strong, which can also broaden the proton rapidity distributions. However we do not use the protons alone to determine the absolute magnitude of the collective motion. Rather we compare multiple particle species from the same collisions simultaneously, to determine the degree of collectivity and the effect of nuclear transparency is expected to be minimal.

#### IV. SUMMARY

In this paper, we have studied the kinetic freeze out conditions of bulk hadrons in central Au + Au and Pb + Pb collisions, at AGS, SPS and partially at RHIC BES energies, using a non boost-invariant version of the blast wave model. Introducing a dependence of the transverse size of the fireball on the longitudinal co-ordinate, the assumption of boost-invariance is explicitly broken. The double differential transverse momentum spectra for a variety of particle species are simultaneously analysed.

The overall fit to the data is reasonably good over a wide range of beam energy. The results indicate a relatively low  $T_{kin}$  in the range 55–90 MeV with a substantial  $\langle\beta_T\rangle$  of about 0.55c – 0.6c. We also found that  $T_{kin}$  increases gradually with the incident beam energy. To explore the effect of longitudinal dynamics, the available rapidity spectra were also analysed. The  $\eta_{\max}$  values showed monotonically increasing trend from AGS to SPS energies. Higher values of  $\eta_{\max}$  was observed in case of elliptic fireball than cylindrical one. This may be attributed to the fact that one needs a larger value of  $\eta_{\max}$  for ellipsoidal cross-section compared to the cylindrical one, in order to have identical volume of the fireball needed to reproduce the measured rapidity spectra. For the upcoming experiments at FAIR and NICA accelerator facilities, these measurements would be useful to better understand the freeze out conditions.

In addition to two freeze-out scenarios, with chemical freeze out preceding the thermal freeze-out, the so called single freeze-out models are also available in literature, both for boost-invariant [37] as well as non boost-invariant longitudinal dynamics [38]. In this model the decays of the resonances as well as the transverse flow change the spectra of the primordial particles in such a way that it is possible to describe well the spectra and the ratios with a single value of the temperature. The basic effect here is that the hadronic decays lead to effective cooling of the spectra. It will be interesting to analyse the present dataset within the single freeze-out scenario in future.

#### V. ACKNOWLEDGEMENT

We would like to thank Premomoy Ghosh, Sushant Singh and Ralf Auerbeck for critically reading the manuscript. P. P. B. is grateful to Kai Schweda and Anton Andronic for illuminating discussions on blast wave model. A.J. is supported in part by the DST-INSPIRE faculty award under Grant No. DST/INSPIRE/04/2017/000038.

- 
- [1] W. Florkowski, Acta Phys. Polon. B **45**, no. 12, 2329 (2014).
  - [2] Ulrich W. Heinz, arXiv:hep-ph/0407360.
  - [3] P. Braun-Munzinger and J. Wambach, Rev. Mod. Phys. **81**, 1031 (2009).
  - [4] J. Adams *et al.* [STAR Collaboration], Nucl. Phys. A **757** (2005), 102.
  - [5] K. Adcox *et al.* [PHENIX Collaboration], Nucl. Phys. A **757** (2005), 184.
  - [6] K. Aamodt *et al.* [ALICE Collaboration], Phys. Rev. Lett. **107** (2011), 032301.
  - [7] G. Aad *et al.* [ATLAS Collaboration], Phys. Rev. C **86** (2012), 014907.
  - [8] S. Chatrchyan *et al.* [CMS Collaboration], Phys. Rev. C **89** (2014), 044906.
  - [9] E. Shuryak, Rev. Mod. Phys. **89** (2017) 035001; U. Heinz, C. Shen and H. Song, AIP Conf. Proc. **1441** (2012) 766.
  - [10] T. Ablyazimov *et al.* [CBM Collaboration], Eur. Phys. J. A **53**, no. 3, 60 (2017).
  - [11] V. Toneev, PoS CPOD **07**, 057 (2007).
  - [12] T. Hirano, N. V. Kolk and A. Bilandizc, Lect. Notes Phys. **785**, 139 (2010); Amaresh Jaiswal and Victor Roy, Advances in High Energy Physics, vol. 2016, Article ID 9623034, 39 pages, 2016.
  - [13] D. Teaney, J. Lauret and E. V. Shuryak, Phys. Rev. Lett. **86** (2001) 4783; B. R. Schlei, D. Strottman and N. Xu, Phys. Rev. Lett. **80** (1998) 3467.
  - [14] W. Florkowski and W. Broniowski, Acta Phys. Polon. B

- 35**, 2895 (2004); W. Florkowski, Nucl. Phys. A **774**, 179 (2006).
- [15] P. J. Siemens and J. O. Rasmussen, Phys. Rev. Lett. **42** (1979) 880.
- [16] K. S. Lee and U. Heinz, Z. Phys. C - Particles and Fields **43** (1989) 425.
- [17] K. S. Lee, U. Heinz and E. Schnedermann, Z. Phys. C - Particles and Fields **48** (1990) 525.
- [18] E. Schnedermann, J. Sollfrank, U. Heinz, Phys. Rev. C **48** (1993) 2462.
- [19] P. Huovinen *et al.*, Phys. Lett. B **503** (2001) 58.
- [20] C. Adler *et al.* STAR Collaboration, Phys.Rev.Lett. **87** (2001) 182301 .
- [21] P. Ghosh, S. Muhuri, J. K. Nayak and R. Varma, J. Phys. G **41**, 035106 (2014) doi:10.1088/0954-3899/41/3/035106 [arXiv:1402.6813 [hep-ph]].
- [22] D. Teaney, Phys. Rev. C **68** (2003) 034913.
- [23] A. Jaiswal and V. Koch, J. Phys. Conf. Ser. **779**, no. 1, 012065 (2017).
- [24] H. Dobler, J. Sollfrank and U. Heinz, Phys. Lett. B **457** (1999) 353.
- [25] F. Cooper and G. Frye, Phys. Rev. D **10**, 186 (1974).
- [26] D. Teaney, J. Lauret and E. V. Shuryak, nucl-th/0110037.
- [27] S. Chapman, J.R. Nix, Phys. Rev. C **54** (1996) 866; J.R. Nix, Phys. Rev. C **58** (1998) 2303.
- [28] J. Sollfrank, P. Koch, U. W. Heniz, Phys. Lett. **B252**(1990) 256; *ibid* Z. Phys. C**52** (1991) 593.
- [29] J. L. Klay *et al.* [E-0895 Collaboration], Phys. Rev. C **68**, 054905 (2003)
- [30] J. L. Klay *et al.* [E895 Collaboration], Phys. Rev. Lett. **88**, 102301 (2002)
- [31] L. Adamczyk *et al.* [STAR Collaboration], Phys. Rev. C **96**, no. 4, 044904 (2017)
- [32] C. Alt *et al.* NA49 Collaboration, Phys.Rev. C**77** (2008) 024903, 2008 .
- [33] S. V. Afanasiev *et al.* NA49 Collaboration, Phys.Rev. C**66** (2002) 054902, 2002 .
- [34] C. Alt *et al.* NA49 Collaboration, Phys.Rev. C**68** (2003) 034903.
- [35] S. Chatterjee *et al.*, Adv. High Energy Phys. **2015** (2015) 349013.
- [36] P. K. Netrakanti and B. Mohanty, Phys. Rev. C **71**, 047901 (2005).
- [37] W. Broniowski and W. Florkowski, Phys. Rev. Lett. **87**, 272302 (2001) ; *ibid* Phys. Rev. C**65** (2002) 064905.
- [38] I. G. Bearden *et al.* [BRAHMS Collaboration], Phys. Rev. Lett. **94**, 162301 (2005).